

Cosmological Implications of a Scalar Field Dark Matter Model

Qinyuan Zheng
Yale University, New Haven, CT

December 12, 2023

ABSTRACT

Scalar field has been used to describe the Dark Matter. The simplest of such models is a real, ultra light scalar field minimally coupled to other components of the universe gravitationally. In this paper, we explore how different density fractions, masses and potentials of such scalar fields impact the cosmological observables using Boltzmann simulation. Two forms of potentials are considered: $V(\phi) = \frac{1}{2}m_\phi^2\phi^2$, $V(\phi) = m_\phi^2f^2[1 + \cos(\phi/f)]$. To match potential real-world cosmology, a three-scalar DM model with particular masses is also considered and compared to Λ CDM model and a two-scalar model. We find that a scalar field dark matter (SFDM) model can reproduce large scale Λ CDM cosmology and give rise to favorable modifications at small scales.

Key words. dark matter - multi scalar field - cosmology

1 Introduction

Λ CDM is the most widely used cosmological model that describes dark matter as cold dark matter (CDM). To be more specific, CDM has the assumed properties of being neutral, non-relativistic, and pressureless. Although many cosmological observations agree with the prediction of this model, some phenomena remain unexplained. To name a few, Λ CDM seems inadequate in the central density behavior in galactic halos or the overpopulation of substructures at small scales [1][2], and the problem of too many satellites rather than a Missing Satellite Problem (MSP) that is raised recently [3]. The inconsistency of Λ CDM with observations almost exclusively arise at relatively small scale, where several attempts have been made to explain away the apparent contradiction. Conceptually there are three main categories of solutions. First, there could be underexplored baryonic dynamics, such as the heating of intergalactic gas by the UV photoionizing background and interaction with supernovae and stellar winds. These dynamics could alter the halo formation process and in certain situations match the observations. On top of that, people have considered modifying the Newtonian force law at certain mass scales, and such models are usually called Modified Newtonian Dynamics (MOND). Finally comes the approach where an alternative dark matter model is proposed. Some representatives include warm dark matter (WDM), self interacting dark matter (SIDM), and exotic braneworld models, etc. Since two decades ago, a scalar field dark matter model (SFDM) has been proposed to tackle these problems [4][5]. In this model, dark matter is either entirely described by the scalar field ϕ , or in combination with the cold dark matter. Previous work has shown that a scalar field with a convex potential behaves like dust at lower redshifts and reproduces the cosmology of CDM. The early time behaviors, on the other hand, could be very different. Preliminary fitting

with the observational data reveals that such a scalar field has an ultra-light mass $\sim 10^{-22}eV$, which forms Bose-Einstein condensates (BEC) at $T_c \sim m^{-5/3} \sim TeV$ at very early time of Universe. These BEC drops are then identified with the galactic halos. At the same time, the Compton wavelengths of the scalar field particles are $\lambda_c = 2\pi\hbar/m \sim Kpc$, which match with dark halo size of typical galaxies[6]. The large scale structures of the universe, by contrast, form just like in a CDM model; hence they are reproduced by SFDM. As expected, the SFDM has important implications on the cosmology[7]. For example, the matter power spectrum (MPS) resulting from a SFDM cosmology has a cut-off at small scales, naturally avoiding the issue with the sub-structures in clusters of galaxies; SFDM cosmology forms galaxies earlier than the CDM cosmology, since an ultralight scalar field has a very high T_c to form BEC halos, which indicates big galaxies at high redshifts with similar characteristics; with the aforementioned mass, the critical mass of collapse for a real scalar field matches the one observed in galaxy halos; the observed properties of dwarf galaxies, including the minimum length scale, the minimum mass scale, and their independence from the brightness, can be reasonably explained by the SFDM cosmology; the SFDM with the aforementioned mass predicts DM halos that have large enough cores to account for the longevity of the cold clump in Ursa Minor and the wide distribution of globular clusters in Fornax, etc.

However, recent work has pointed out in order to better fit the cosmological observations, the scalar field dark matter may need to have different masses at different scales in simulations. As a result, it seems a good resolution to extend SFDM to a multi scalar field dark matter model. There are a few other motivations to extend this model to a multi field one. First, the dark matter particles can exist in multiple quantum states, giving them different effective potentials if the original mass is light. Second, the dark matter could be made of multi-

ple species to begin with, just as the baryonic counterpart does. Moreover, a single scalar field model does fall short in describing some observations, requiring different masses on different scales. We consider two convex potential forms here[8]: 1. a free scalar field; 2. an axion potential $m_{\phi_i}^2 f_i^2 [1 + \cos(\phi_i/f_i)]$. The free theory is the simplest and most natural convex potential form. The physical motivation of 2. can be traced back to the non-perturbative effects in QCD which generate a periodic behavior after the breaking of the Peccei-Quinn symmetry $U(1)_{PQ}$ due to instantons. Alternatively it could come from compactification of extra dimensions in string theories. [9][10][11][12]

Recent study of structure formation [13] has hinted at a dark matter model where three scalar fields of different mass scales $\sim 10^{-22} \text{eV}$, $\sim 10^{-20} \text{eV}$, $\sim 10^{-18} \text{eV}$ are present simultaneously. Although the third field is expected to have a very small initial DM density fraction, it is interesting to see how a third field with non-negligible DM density fraction could alter the cosmology. In particular, a three-field DM model is a first step of generalization to a many-field DM model from a two-field DM model. Whether some of the features of two-scalar model persist or change should be useful information for better understanding of SFDM theories.

The paper is structured as follows. In section II we present the analytic details of the background evolution and density linear perturbation of the model. In section III a modified CLASS code is used to study the mass power spectrum, CMB power spectrum and background density of first a one-scalar DM model, and then a three-scalar SFDM model in terms of different field contributions. In section IV we summarize the overall findings and address the future directions.

2 Analytic Analysis

For this project we assume a flat universe filled with the standard components: baryons, dark energy (cosmological constant Λ), radiation, and dark matter. The dark matter is described by multiple scalar fields, in combination with CDM.

2.1 Background Evolution

In the numerical solution, we investigate a cosmology with three dark matter scalar field species. However, this analysis below works for any number of dark matter fields. To further simplify the analysis, we assume real DM scalar fields with no mutual interactions. In a FLRW metric, the action describing the DM field is

$$S = \int d^4x \sqrt{-g} \left(-\frac{1}{2} g^{\mu\nu} \nabla_\mu \phi \nabla_\nu \phi - \frac{1}{2} m^2 \phi^2 \right) \quad (1)$$

where the ∇ 's are covariant derivative. In FLRW metrix, the metric tensor takes the form

$$g_{\mu\nu} = (1, -a^2, -a^2, -a^2) \quad (2)$$

where a is the scale factor. Thus the Klein-Gordon equation of motion becomes

$$\frac{1}{a^3} \partial_\mu (a^3 g^{\mu\nu} \partial_\nu \phi) = -\partial_\phi V(\phi) \quad (3)$$

plugging in $H = \dot{a}/a$, we have

$$\ddot{\phi}_i = -3H\dot{\phi}_i - \partial_{\phi_i} V(\phi_i) \quad (4)$$

where the subscripts i 's denote different scalar fields, the dots represent derivatives with respect to the cosmic time t . The scalar fields are evolved merely through the Klein-Gordon equation coupled with the usual Friedmann equation and Euler equations describing the rest matter components treated as perfect fluids. Thus the complementary equations

$$\dot{\rho}_I = -3\frac{\dot{a}}{a}(\rho_I + p_I) \quad (5)$$

$$H^2 = \frac{\kappa^2}{2} \left(\sum_I \rho_I + \sum_i \rho_{\phi_i} \right) \quad (6)$$

where I denote the matter components other than the SFDM, $\kappa^2 = 8\pi G$.

For scalar fields, the energy density and pressure are given by

$$\rho_{\phi_i} = (1/2) \dot{\phi}_i^2 + V_i(\phi_i) \quad (7)$$

$$p_{\phi_i} = (1/2) \dot{\phi}_i^2 - V_i(\phi_i) \quad (8)$$

Following the convention of [14], one can introduce a polar transformation for ease of numerics:

$$\frac{\kappa \dot{\phi}_i}{\sqrt{6}H} = \Omega_{\phi_i}^{1/2} \sin(\theta_i/2), \quad \frac{\kappa V_i^{1/2}}{\sqrt{3}H} = \Omega_{\phi_i}^{1/2} \cos(\theta_i/2) \quad (9)$$

where $\Omega_{\phi_i} = \kappa^2 \rho_{\phi_i} / 3H^2$ is the dimensionless density parameter, θ_i is related to the equation of state for each scalar field with $w_{\phi_i} = p_{\phi_i} / \rho_{\phi_i} = -\cos(\theta_i)$.

As aforementioned, we will focus on two potential forms and their possible combinations:

$$V_i(\phi_i) \begin{cases} m_{\phi_i}^2 f_i^2 [1 + \cos(\phi_i/f_i)] \\ (1/2) m_{\phi_i}^2 \phi_i^2 \end{cases} \quad (10)$$

where f_i is a characteristic energy scalar for the scalar field, and m_{ϕ_i} is the corresponding mass scale.

We can further define the potential variables y_{1i} and y_{2i} as

$$y_{1i} = -2\sqrt{2} \frac{\partial_{\phi_i} V_i^{1/2}}{H}, \quad y_{2i} = -4\sqrt{3} \frac{\partial_{\phi_i}^2 V_i^{1/2}}{\kappa H} \quad (11)$$

Plugging back in (4), we have

$$y_{1i}^2 = 4 \frac{m_{\phi_i}^2}{H^2} - 2\lambda_{\phi_i} \Omega_{\phi_i} \quad (12)$$

$$y_{2i} = \lambda_{\phi_i} y_{1i} \quad (13)$$

where $\lambda_{\phi_i} = 3/\kappa^2 f_i^2$. Positive values of λ_{ϕ_i} describe the cosine potential, and $\lambda_{\phi_i} = 0$ describes the quadratic potential. [15][16] Now the Klein-Gordon equation can be

greatly simplified for the convenience of numerical solution, represented by a set of equations

$$\theta'_i = -3\sin\theta_i + y_{1i} \quad (14)$$

$$\Omega'_{\phi i} = 3(w_{tot} + \cos\theta_i)\Omega_{\phi i} \quad (15)$$

$$y'_{1i} = \frac{3}{2}(1 + w_{tot})y_{1i} + \frac{1}{2}\lambda_{\phi i}\Omega_{\phi i}^{1/2}\sin\theta_i \quad (16)$$

where $w_{tot} = \sum \Omega_I w_I + \sum \Omega_i w_i$, and primes denote the derivatives with respect to the number of e-folds $N = \ln a$, where it is easy to show that for any given variable q then $\dot{q} = Hq'$.

2.2 Linear Density Perturbation

In this project we consider the linear perturbations for the scalar fields

$$\phi_i(x, t) = \phi_i(t) + \psi_i(x, t) \quad (17)$$

where total field strength is written in terms of the background field $\phi_i(t)$ and the linear perturbation $\psi_i(x, t)$.

$$\delta'_{0i} = -[3\sin\theta_i + \frac{k^2}{k_{Ji}^2}(1 - \cos\theta_i)]\delta_{1i} + \frac{k^2}{k_{Ji}^2}\sin(\theta_i)\delta_{0i} - \frac{1}{2}h'(1 - \cos\theta_i) \quad (23)$$

$$\delta'_{1i} = -[3\cos\theta_i + (\frac{k^2}{k_{Ji}^2} - \frac{\lambda_{\phi i}\Omega_{\phi i}}{2y_{1i}})\sin\theta_i]\delta_{1i} + (\frac{k^2}{k_{Ji}^2} - \frac{\lambda_{\phi i}\Omega_{\phi i}}{2y_{1i}})(1 + \cos(\theta_i)\delta_{0i} - \frac{1}{2}h'\sin\theta_i) \quad (24)$$

where $k_{Ji}^2 = H^2 a^2 y_{1i}$. At this point, we can also calculate the following quantities in terms of the new variables

$$\delta\rho_{\phi i} = \dot{\phi}_i\dot{\psi}_i + \partial_{\phi i}V\psi_i = \delta_{0i}\rho_{\phi i} \quad (25)$$

$$\delta p_{\phi i} = \dot{\phi}_i\dot{\psi}_i - \partial_{\phi i}V\psi_i = (\delta_{1i}\sin\theta_i - \delta_{0i}\cos\theta_i)\rho_{\phi i} \quad (26)$$

$$(\rho_{\phi i} + p_{\phi i})\Theta_{\phi i} = \frac{k^2}{a}\dot{\phi}_i\psi_i = \frac{k^2\rho_{\phi i}}{aHy_{1i}}[(1 - \cos\theta_i)\delta_{1i} - \sin\theta_i\delta_{0i}] \quad (27)$$

where $\delta\rho_{\phi i}$ is the density perturbation, $\delta p_{\phi i}$ is the pressure perturbation, and $\Theta_{\phi i}$ is the velocity divergence.

3 Numerical Solutions

In this section we present the background evolution, mass power spectrum, CMB power spectrum, and extrapolated halo mass function of different combination of potentials and distribution of density fractions among scalar fields of different masses. Because a multi-field case can be written as a single field with an effective mass given the same potential form with possible individual field dynamics ignored, a single field DM simulation can lend us insight into how a scalar field DM behaves. Hence we start with a single field calculation with varying parameters. Finally, we extend the modified CLASS code to calculate a three-scalar field case. The initial conditions are fixed by matching the initial values of the dynamical quantities $(\theta_i, y_{1i}, \Omega_{\phi i})_{ini}$ with the present density parameters

The perturbed metric in the synchronous gauge is $ds^2 = -dt^2 + a^2(t)(\delta_{lm} + h_{lm})dx^l dx^m$, h_{lm} being the tensor perturbations of the metric. The perturbed KG equation becomes in Fourier space

$$\ddot{\psi} = -3H\dot{\psi}_i - (\frac{k^2}{a^2} + \partial_{\phi i}^2 V_i)\psi_i - \frac{1}{2}\dot{h}\dot{\phi}_i \quad (18)$$

where k is the comoving wavenumber, h is the trace of h_{lm} . Similar to what has been done with the background scalar field, we have

$$\sqrt{\frac{2}{3}}\frac{\kappa\dot{\psi}}{H} = -\Omega_{\phi i}^{1/2}e^{\alpha_i}\cos(\frac{v_i}{2}) \quad (19)$$

$$\frac{\kappa y_{i,1}\dot{\psi}_i}{\sqrt{6}} = -\Omega_{\phi i}^{1/2}e^{\alpha_i}\sin(\frac{v_i}{2}) \quad (20)$$

where α_i and v_i are defined as

$$\delta_{0i} = -e^{\alpha_i}\sin(\frac{\theta_i - v_i}{2}) \quad (21)$$

$$\delta_{1i} = -e^{\alpha_i}\cos(\frac{\theta_i - v_i}{2}) \quad (22)$$

and the density contrast $\delta_{\phi i} = \delta\rho_{\phi i}/\rho_{\phi i} = \delta_{0i}$. The KG equation becomes

$\Omega_{\phi i}$. [15][16] The initial linear perturbations are set to zero. The mass scales are $\sim 10^{-22}eV, \sim 10^{-20}eV, \sim 10^{-18}eV$ as reported in [13]. Throughout the numerical study, we adopt the neutrino mass hierarchy where two species are massless and one species is massive with $\sum_\nu m_\nu = 0.06eV$. [17]

For the one-scalar SFDM case, we assume that DM is composed of CDM and one scalar field with a potential specified in eq (10). Define $R = \Omega_{sf,0}/\Omega_{DM,0}$; we consider $R = 0, 0.5, 1$ for each potential form. For a broader sweep in the parameter space, we present the results of $m \sim 10^{-18}, 10^{-22}, 10^{-26}eV$. For each mass scale, two potential forms are considered. Both linear mass power spectrum and CMB power spectrum are presented for each case.

Let us make some general observations before delv-

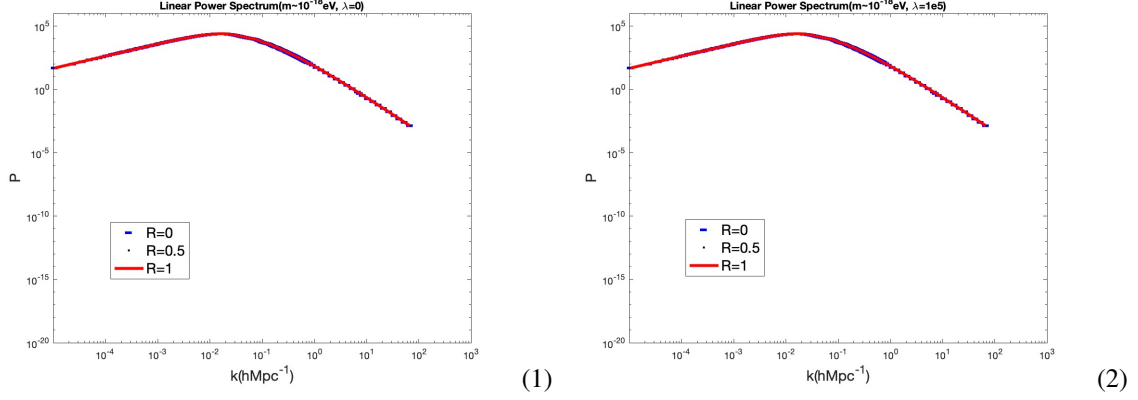


Figure 1: Linear Power Spectrum for $m \sim 10^{-18} \text{eV}$ scalar field DM with varying potentials and density fractions at $z=0$. (1)quadratic potential; (2)axion-like cos potential.

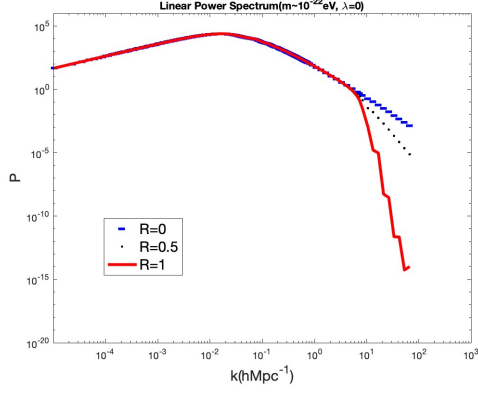
ing into the detailed dependence on mass scale, density distribution and potential form. The most obvious signature of a SFDM model is the cut-off at small scale in the mass power spectrum (MPS). The MPS for any intermediate R value is bounded by MPS for $R = 0$ and $R = 1$. On the other hand, the SFDM preserves the CMB power spectrum of ΛCDM to high accuracy, only with noticeable deviation when the mass scale of the scalar field becomes really small ($m \sim 10^{-26} \text{eV}$).

Investigating the dependence on mass scale of the scalar field, we can see that the smaller the mass is, the larger scale the cut-off in the MPS begins at, and the more steep the cut-off becomes. For $m \sim 10^{-26} \text{eV}$, the cut-off scale is roughly $0.1 h\text{Mpc}^{-1}$; for $m \sim 10^{-22} \text{eV}$, the cut-off scale reduces to about $4 h\text{Mpc}^{-1}$; at $m \sim 10^{-18} \text{eV}$, the cut-off does not happen at all within the plotted scales. (Notice that large scale here is corresponding to smaller k .) This makes sense because when the scalar field is heavy enough, it is essentially dust-like, reproducing the behavior of ΛCDM model. The quadratic and cos potentials have similar behaviors in mass power spectrum, while the quadratic potential does a slightly better job at preserving the CMB power spectrum when mass scale and density fraction are held same.

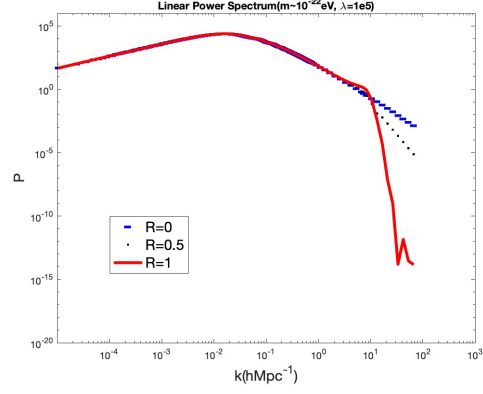
To match cosmological observations, we also calculate the Press-Schechter halo mass function for quadratic potential with $m \sim 10^{-22} \text{eV}$, 10^{-20}eV , 10^{-18}eV . For reference, they are shown together in figure(7) normalized to the PS halo mass function of ΛCDM . It can be seen that with decreasing mass scale of the scalar field, there is a tendency of fewer halos at large halo mass scale. However, among the three masses presented here, only $m \sim 10^{-22} \text{eV}$ has a pronounced effect of suppressed halo number at large mass. It can also be seen that at very high halo mass scale, $m \sim 10^{-18} \text{eV}$ and $m \sim 10^{-20} \text{eV}$ have a bump which predicts a higher halo number than the ΛCDM . This effect exists for other lower mass SFDM, but it is unclear whether this is real or numerical. For further investigation, one can set up a many-body simulation to verify.

To gauge how a three-scalar DM could alter the cos-

mology, we present a comparison study of 1) ΛCDM ; 2) two-scalar DM with $m_{\phi 1} = 10^{-22} \text{eV}$, $m_{\phi 2} = 10^{-20} \text{eV}$, and $R_{\phi 1} = 0.8, R_{\phi 2} = 0.2$; 3) three-scalar DM with $m_{\phi 1} = 10^{-22} \text{eV}$, $m_{\phi 2} = 10^{-20} \text{eV}$, $m_{\phi 3} = 10^{-18} \text{eV}$, and $R_{\phi 1} = 0.8, R_{\phi 2} = 0.16, R_{\phi 3} = 0.04$. For the scalar fields, quadratic potential is used. As expected, we notice a cut-off at small scale ($k \sim 4 h\text{Mpc}^{-1}$) in the linear power spectrum. The 3 component SFDM cut-off begins at a larger scale but the 2 component SFDM cut-off is steeper, thus producing a cross over in the MPS. This behavior is not unexpected owing to our 1 component SFDM analysis, where we note that larger mass of the scalar field results in a less steep cut-off in MPS. This observation grants us flexibility to tune the mass parameters (and their density fractions) to account for different cosmological constraints at different scales. Both the two component and the three component SFDM reproduce the ΛCDM CMB power spectrum to very high accuracy. When plotted normalized with respect to the ΛCDM case, we see that the 3 component SFDM case oscillates more than 2 component case, while on average the 2 component case deviates more from the ΛCDM case. In figure 10 we plot the dark matter density evolution normalized with respect to the ΛCDM model. We can see that in the three component SFDM model DM oscillates with a larger amplitude than in two component SFDM, and the fluctuation damps down later in the three component SFDM model as well. Finally, perhaps a little counter-intuitively, we find that the 3 component SFDM model predicts a larger drop in halo number at relatively high halo mass than the 2 component SFDM model, compared to the standard ΛCDM cosmology. This result should be taken with a grain of salt due to the ultra light mass of the scalar field DM particles. The growth factor should be suppressed on small scales because of the free-streaming of the SFDM. Reflected in the halo mass function, this should induce an increase in the critical overdensity for halos of smaller masses, contrary to the constant in the ΛCDM model. However, this does not influence our observation for large halo mass limit. We leave the investigation of this intricacy to future work.

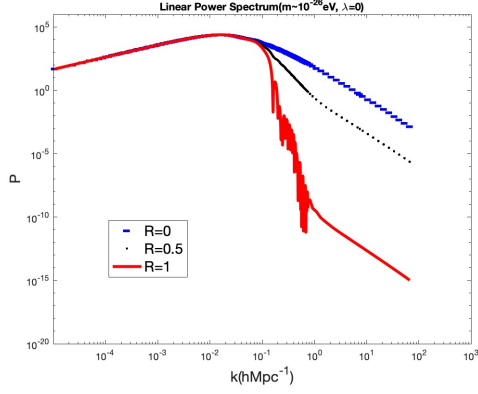


(1)

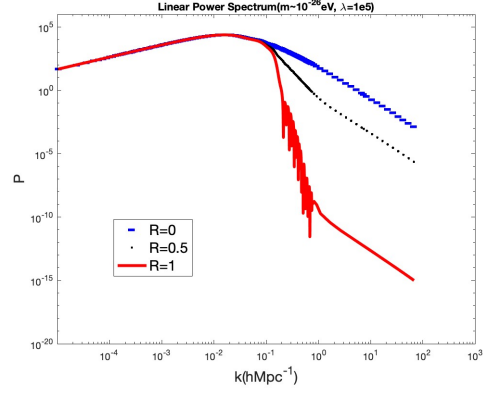


(2)

Figure 2: Linear Power Spectrum for $m \sim 10^{-22} eV$ scalar field DM with varying potentials and density fractions at $z=0$. (1)quadratic potential; (2)axion-like cos potential.

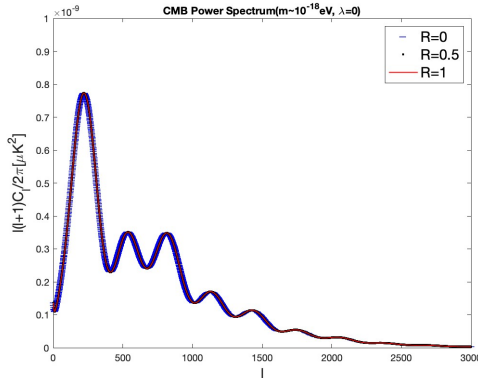


(1)

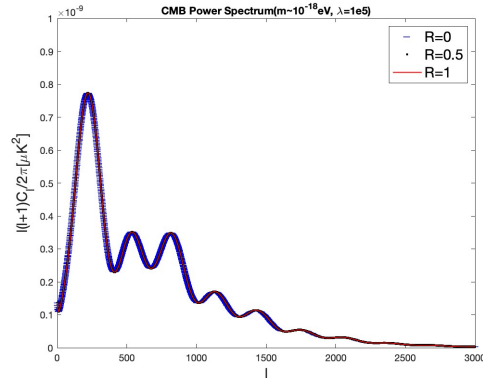


(2)

Figure 3: Linear Power Spectrum for $m \sim 10^{-26} eV$ scalar field DM with varying potentials and density fractions at $z=0$. (1)quadratic potential; (2)axion-like cos potential.

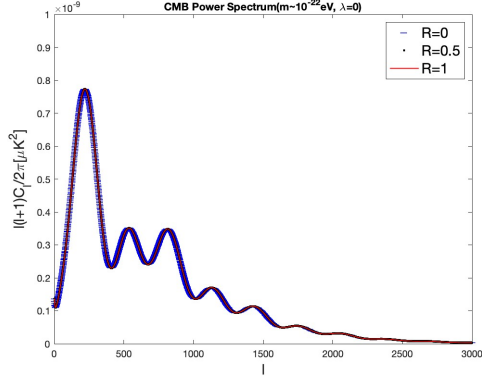


(1)

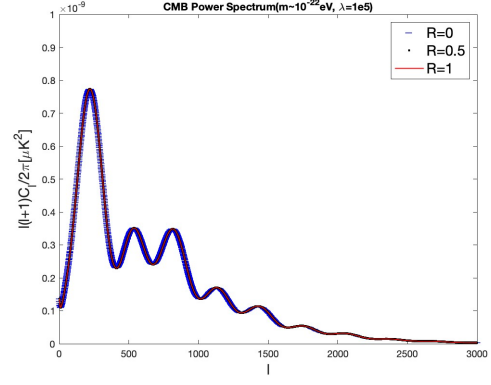


(2)

Figure 4: CMB Spectrum for $m \sim 10^{-18} eV$ scalar field DM with varying potentials and density fractions. (1)quadratic potential; (2)axion-like cos potential.

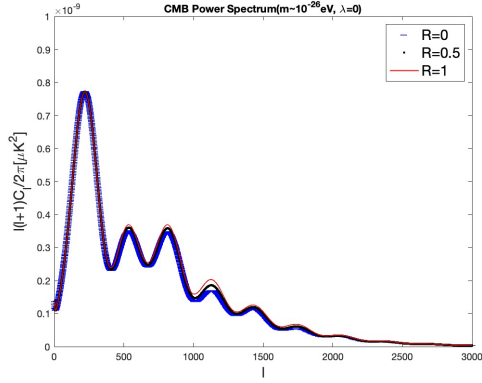


(1)

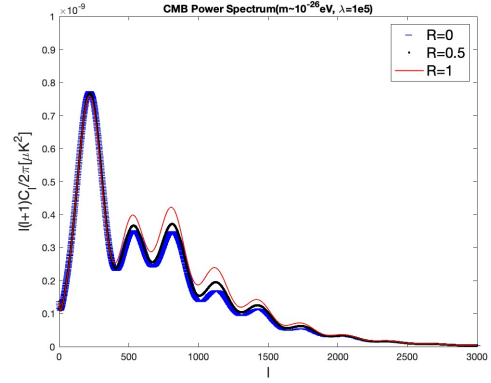


(2)

Figure 5: CMB Spectrum for $m \sim 10^{-22} eV$ scalar field DM with varying potentials and density fractions. (1)quadratic potential; (2)axion-like cos potential.



(1)



(2)

Figure 6: CMB Spectrum for $m \sim 10^{-26} eV$ scalar field DM with varying potentials and density fractions. (1)quadratic potential; (2)axion-like cos potential.

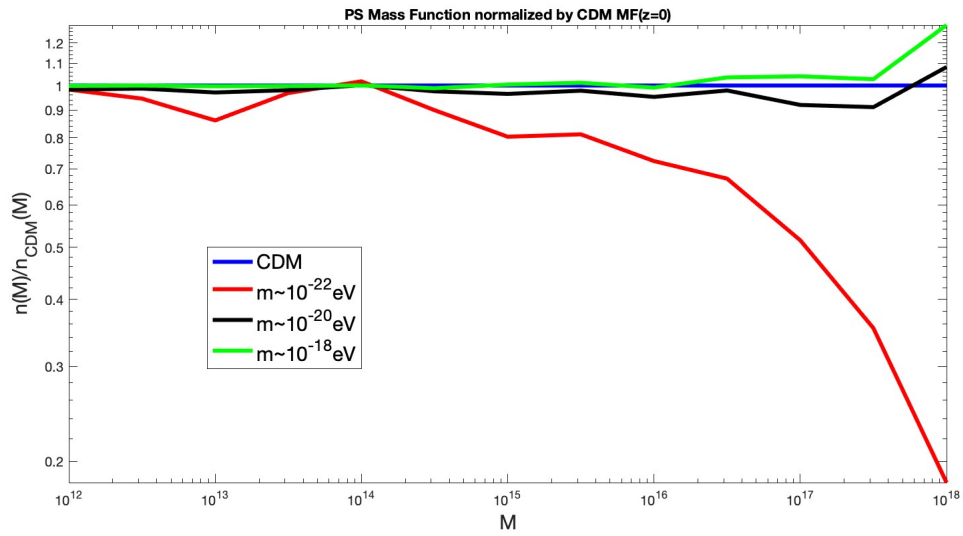


Figure 7: Press-Schechter Halo Mass Function for scalar field DM of different masses with quadratic potential normalized by the CDM mass function

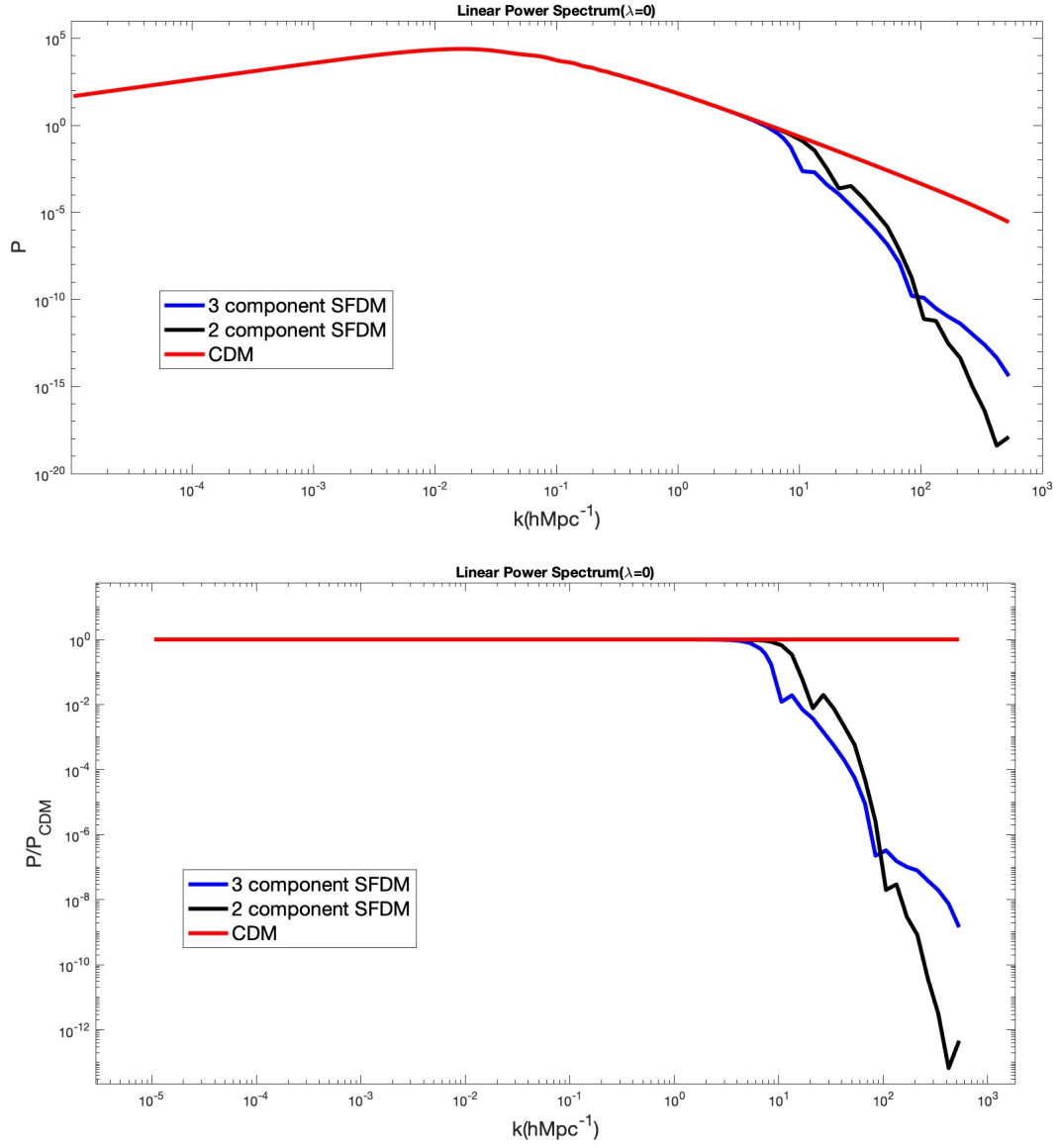


Figure 8: Linear Power Spectrum of the 3-scalar and 2-scalar cases with ΛCDM as reference.

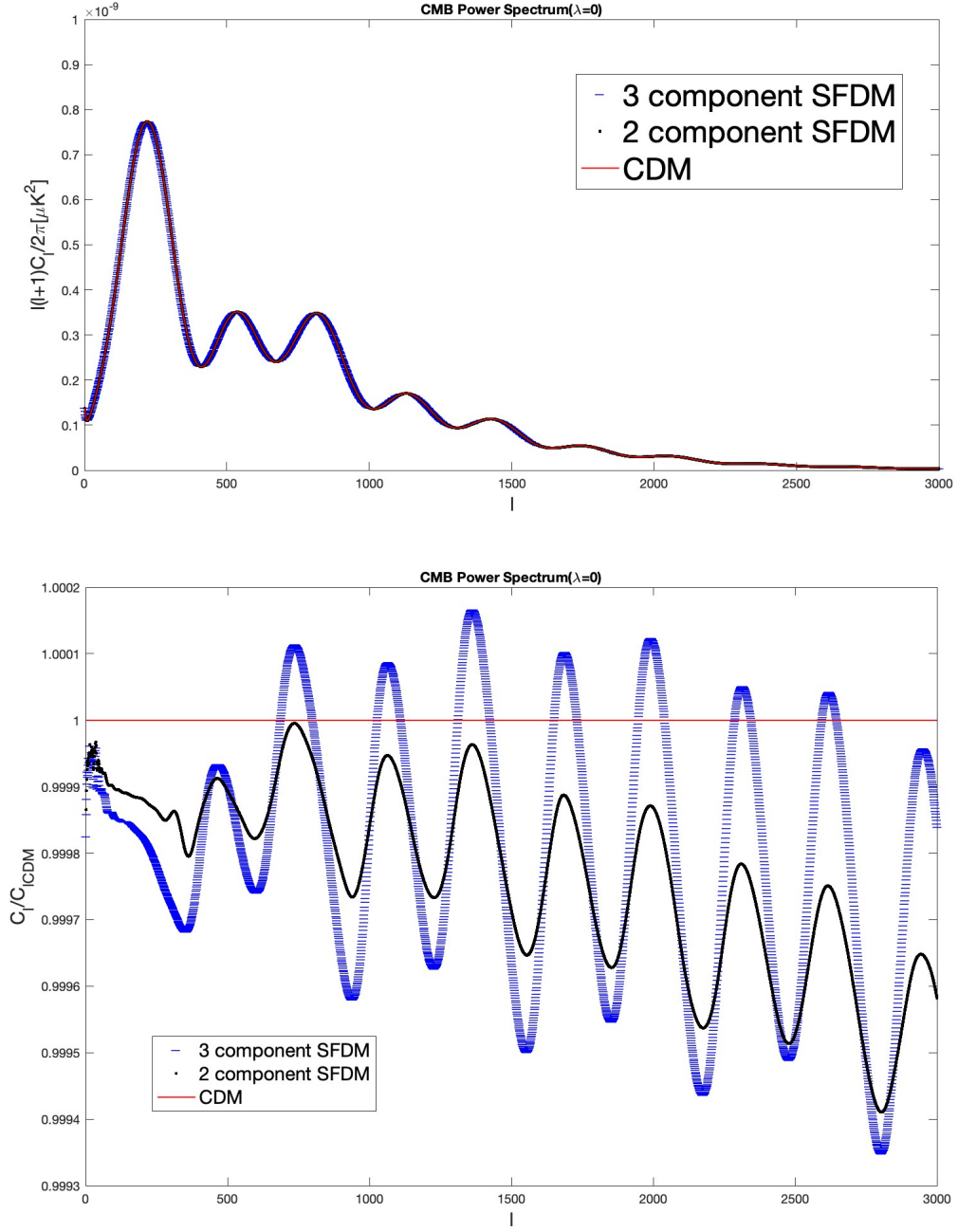


Figure 9: CMB Power Spectrum of the 3-scalar and 2-scalar cases with Λ CDM as reference.

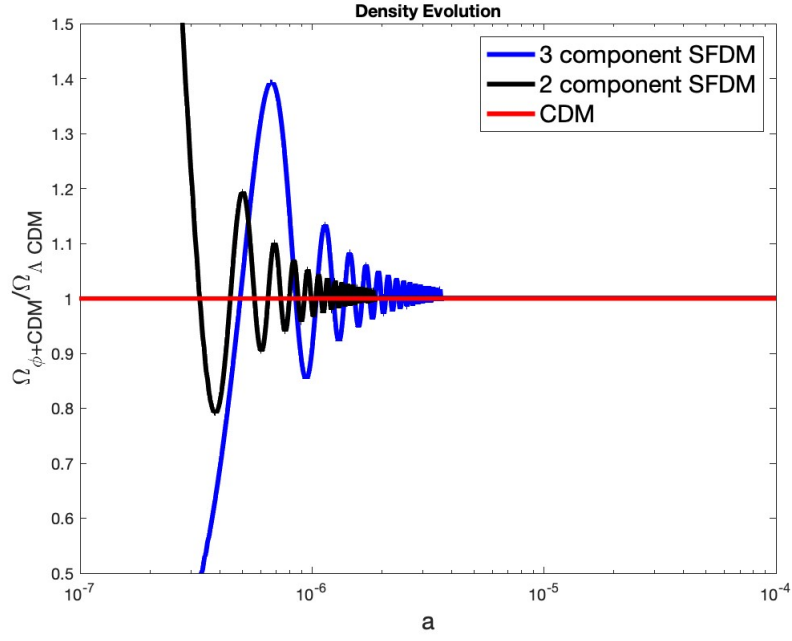


Figure 10: DM density evolution of the 3-scalar and 2-scalar case with Λ CDM as reference.

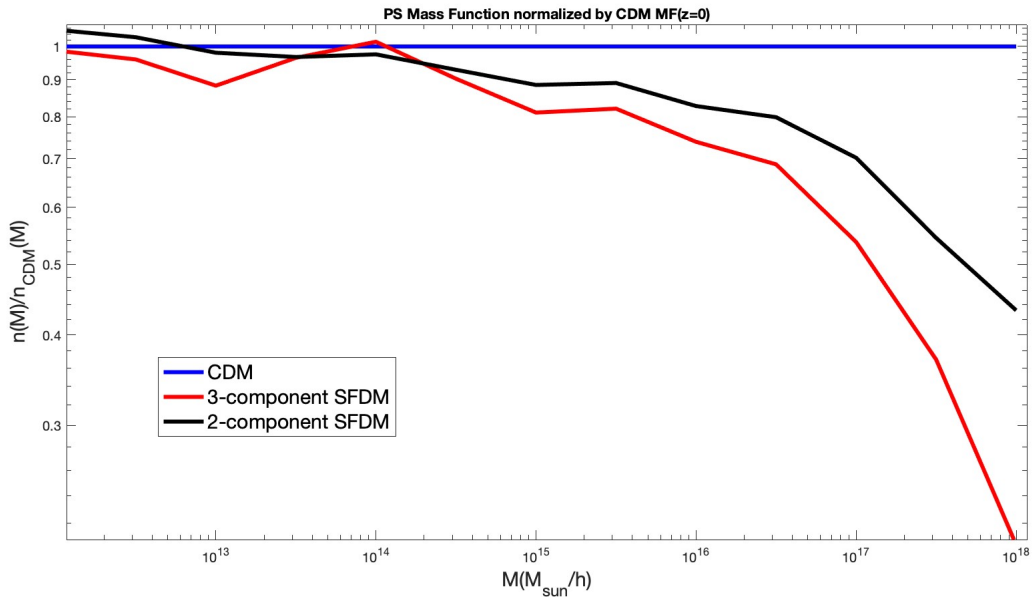


Figure 11: Halo mass function normalized with respect to the Λ CDM.

4 Conclusions

In this work we presented some cosmological implications of scalar field dark matter model, where dark matter is assumed to be entirely or partially made up of ultralight scalar fields. We limit our work to real scalar fields, and investigate the dependence on field mass, field potential form and field density fraction. To manifest the cosmological implications, we present linear mass power spectrum, CMB power spectrum and halo mass function of various scenarios. It turns out that SFDM can reproduce results of Λ CDM model pretty accurately at large scales, and give us a tuning knob for explaining small scale observations that appear incompatible with Λ CDM. In re-

sponse to motivation of a three-component SFDM model derived from both theoretical and observational study in the structure formation, we also explore the cosmological imprints of a three-component SFDM with educated assumption on their masses and density fractions, and compare it with a two-component SFDM as well as the Λ CDM model. We comment on some interesting features of such models and invite future discussion and applications. There are a few ideas that we leave unexplored for now in this work. For example, one can include mutual interactions between the different scalar fields; one can also consider complex scalar fields; with the observational data, one can use Monte Python code [18] to constrain the scalar field dark matter model parameters. These will be done in following work.

5 References

- [1] D.H. Weinberg, J.S. Bullock, F. Governato, R. Kuzio de Naray and A.H.G. Peter, Cold dark matter: controversies on small scales, *Proc. Nat. Acad. Sci.* 112
- [2] P. Bull et al., Beyond Λ CDM: Problems, solutions, and the road ahead, *Phys. Dark Univ.* 12 (2016) 56 [1512.05356].
- [3] DES collaboration, Milky Way Satellite Census. III. Constraints on Dark Matter Properties from Observations of Milky Way Satellite Galaxies, *Phys. Rev. Lett.* 126 (2021) 091101 [2008.00022].
- [4] S.-J. Sin, Late-time phase transition and the galactic halo as a bose liquid, *Phys. Rev. D* 50 (1994) 3650.
- [5] L. Hui, J.P. Ostriker, S. Tremaine and E. Witten, Ultralight scalars as cosmological dark matter, *Phys. Rev. D* 95 (2017) 043541 [1610.08297].
- [6] T. Matos and F.S. Guzman, Scalar fields as dark matter in spiral galaxies, *Class. Quant. Grav.* 17 (2000) L9
- [7] J. Magana and T. Matos, A brief Review of the Scalar Field Dark Matter model, in *Journal of Physics Conference Series*, vol. 378 of *Journal of Physics Conference Series*, p. 012012, Aug., 2012, DOI [1201.6107].
- [8] L. O. Téllez-Tovar, Tonatiuh Matos, J. Alberto Vázquez, Cosmological constraints on the Multi Scalar Field Dark Matter model, *Phys. Rev. D* 106, 123501 (2022).
- [9] T. Matos, A. Vazquez-Gonzalez and J. Magana, Study of several potentials as scalar field dark matter candidates, *AIP Conf. Proc.* 1083 (2008) 144.
- [10] DES collaboration, Milky Way Satellite Census. III. Constraints on Dark Matter Properties from Observations of Milky Way Satellite Galaxies, *Phys. Rev. Lett.* 126 (2021) 091101 [2008.00022].
- [11] L. Hui, J.P. Ostriker, S. Tremaine and E. Witten, Ultralight scalars as cosmological dark matter, *Phys. Rev. D* 95 (2017) 043541 [1610.08297].
- [12] F.X. Linares Cedeno, A.X. Gonzalez-Morales and L.A. Urena Lopez, Ultralight DM bosons with an axion-like potential: scale-dependent constraints revisited, *JCAP* 01 (2021) 051 [2006.05037].
- [13] Hoang Nhan Luu, S. -H. Henry Tye, Tom Broadhurst. Multiple Ultralight Axionic Wave Dark Matter and Astronomical Structures. *Phys. Dark Univ.* 30 (2020) 100636.
- [14] L.A. Urena Lopez, New perturbative method for analytical solutions in single-field models of inflation, *Phys. Rev. D* 94 (2016) 063532 [1512.07142].
- [15] L.A. Urena Lopez and A.X. Gonzalez-Morales, Towards accurate cosmological predictions for rapidly oscillating scalar fields as dark matter, *JCAP* 07 (2016) 048 [1511.08195].
- [16] F.X.L. Cedeno, A.X. Gonzalez-Morales and L.A. Urena Lopez, Cosmological signatures of ultralight dark matter with an axionlike potential, *Phys. Rev. D* 96 (2017) 061301 [1703.10180].
- [17] Planck collaboration, Planck 2018 results. VI. Cosmological parameters, *Astron. Astrophys.* 641 (2020) A6 [1807.06209].
- [18] T. Brinckmann and J. Lesgourgues, MontePython 3: boosted MCMC sampler and other features, *Phys. Dark Univ.* 24 (2019) 100260 [1804.07261].